Engineering Solid Mechanics 12 (2024) 17-26

Contents lists available at GrowingScience

Engineering Solid Mechanics

homepage: www.GrowingScience.com/esm

Investigating the fracture toughness of the self compacting concrete using ENDB samples by changing the aggregate size and percent of steel fiber

Seyed Roohollah Mousavi[a], Mohammad Ghasemi[b*] and Mohammad Dehghani[a]

[a]*Civil Engineering Department, University of Sistan and Baluchestan, Zahedan, Iran*
[b]*Civil Engineering Department, University of Velayat, Iranshahr, Iran*

A R T I C L E I N F O

Article history:
Received 21 May 2023
Accepted 24 July 2023
Available online
24 July 2023

Keywords:
ENDB specimen
Fracture toughness
Self-compacting concrete
Mixed mode I/III
Maximum aggregate size

A B S T R A C T

In reality, concrete structures are normally under various loadings, and results of different studies have shown that cracks in these structures and their materials, due to their nature as well as the loading type, do not develop along the crack plane (pure mode I); rather, they expand under mixed modes, making the crack growth studies under these modes a very important issue. In the crack growth phenomenon, the fracture toughness is a very effective parameter usually calculated by ENDB samples because they are easy to handle. In this study, several samples were made by changing the maximum aggregates size (dmax = 9.5, 12.5 & 19 mm) and the amount of hooked-end steel fibers (SF = 0.1, 0.3 & 0.5%), and tested under different loading modes (pure/mixed modes I and III) using the strain control jack device. According to the results, the lowest fracture toughness belonged to pure mode III, aggregates with dmax = 12.5 mm performed better in the self-compacting concrete reinforced with steel fiber, Also, the results show that the increasing trend of steel fibers does not have a positive effect on the fracture toughness performance.

1. Introduction

The growing trend of using concrete in the construction industry has led to the growth and development of new concrete types, one of which is self-compacting concrete (SCC) that moves in the mold under its own weight with no vibrations, reducing both cost and time; therefore, improving its resistance against impact loads, ductility and energy absorption capacity are important issues to be investigated. (Picazo et al., 2018; Al-Hadithi et al.,2019). Concrete is an admixture material consisting of aggregates, cement, water, additives, and so on. As aggregates occupy a significant part of the concrete and their volume, size, type and distribution have different effects on its properties and fracture behavior, some studies focused on the aggregate volume and showed that an increase in it increased the fracture energy (G_F) and fracture toughness (K_I) (Akcay et al., 2012). Beigi et al. (2014), showed that increasing the aggregate size in the SCC increased the fracture energy, and Sadrmomtaz et al. (2020), reported that increasing the nominal size of the largest aggregate in heavy-aggregate concretes increased the fracture energy and fracture toughness. Ghasemi et al. (2020), reported that increasing the aggregate size up to dmax = 12.5 mm in self-compacting concrete reinforced with steel fiber (SCCF) increased the fracture energy, but larger aggregates disturbed the fracture surface. They also stated that fibers were very effective in the post peak and increased the concrete energy absorption and ductility. Many researchers (Ghasemi et al., 2018; Ferrara et al., 2007; El-Dieb, 2009; Li et al., 2020; Ferdosian & Camoes, 2021; Hoseini et al.,2023; Mousavi et al., 2019) have reported that, besides aggregates and cement paste, fibers to play a vital role in improving the post-cracking fracture energy/toughness in different concretes, and their volume, size and type are among the concrete-fracture influencing parameters.

* Corresponding author.
E-mail addresses: m.ghasemi@Velayat.ac.ir (M. Ghasemi)

ISSN 2291-8752 (Online) - ISSN 2291-8744 (Print)

doi: 10.5267/j.esm.2023.7.006

Fracture mechanics is the science that examines the crack stability and various reasons for its formation in concrete structures. Results of studies carried out, in recent decades, on mode I fracture mechanics (Beygi et al., 2013; Ghasemi et al., 2019; Iqbal et al., 2015; Siddique et al., 2016; Madandoust et al., 2015; Alberti et al.,2015) have shown that cracks in these structures and their materials, due to their nature as well as the loading type, do not develop along the crack plane (pure mode I); rather, they expand under mixed modes. Although fracture under pure modes II and III, and mixed modes I/II and I/III have recently received attention, fracture toughness data for these loading modes are still relatively scarce, and using a simple, inexpensive, reliable sample is a very important factor in developing the lab activities. In the Edge Notch Disc Bend (ENDB) beam sample presented by Aliha et al.(2015), for use in asphalt and concrete tests, the sides of the disc involve mode II cracks and its center contains only modes I and III cracks (mode II cracks are none). This method is recently used by many researchers (Pirmohammad & Bayat, 2016; Haghighat Pour et al., 2018; Aliha et al., 2018; Mansourian et al., 2018; Aliha et al., 2017; Aliha et al., 2016; Haghighatpour & Aliha, 2022; Mousavi et al., 2021; Hoseini et al., 2022); for instance, Pirmohamed et al. (2016), studied the low-temperature fracture toughness of ENDB samples under pure modes I and III and reported that adding mode III to mode I reduced the fracture resistance. Aliha et al. (2018), used ENDB samples to study concretes containing forta-ferro fibers and showed that these fibers affected mode III more than mode I, and FR concretes had better post-peak behavior than normal concretes. Using three disc shape test configurations loaded with tensile, compression and bending methods, Gu et al. (2023) demonstrated that the mode I cracking resistance of concrete materials are highly dependent to both geometry and loading type. Mousavi et al. (2021), examined the effects of waste glass aggregates in concrete and reported that using 20-40% of them improved the fracture toughness; they also showed that the sample age had the highest effects on mode 3 results. Hosseini et al. (2022), studied the effects of the volume of aggregate and wavy steel fibers on the fracture toughness and showed that increasing aggregates increased the fracture toughness. Najjar et al. (2020; 2022 a,b,c; 2023) performed extensive experimental study to characterize mixed mode fracture resistance of cement emulsified asphalt mortar under static and cyclic loads and different environmental conditions such as aging and freeze/thaw cycles. They used SCB and ENDB concrete samples in their studies. Daneshfar et al. (2017; 2022; 2023a,b) assessed the fracture toughness, fracture energy and flexural strength of Macro-Synthetic-Fiber-Reinforced Concrete beams with or without an initial crack in the samples. The effect of fiber size, fiber content and sample size were investigated in the works of Daneshfar and his coworkers. Karimi and coworkers (2023 a,b) used the ENDB specimen to investigate the fracture resistance and fracture energy of cement concrete reinforced with tire rubber granules with different percentages and sizes. They proposed suitable ranges of adding recycled tire rubber powder and granules that can be added to the mixture of control concrete with an acceptable resistance against fracture. Using edge cracked bend beam samples, Rooholamini et al. (2018 a,b) studied experimentally the fracture load and fracture path of growing crack in macro-synthetic fiber reinforced roller-compacted concrete specimens. Other researchers utilized different additives with different shapes, types, contents in the mechanical, strength and fracture properties of different concrete materials such as polymer concrete, asphalt concrete, cement concrete, etc. (Motamedi et al. 2020; Fakhri et al. 2021; He et al. 2022; Aliha et al. 2017, 2022a,b; Karamzadeh et al. 2022; Asdollah-Tabar et al. 2021; Karimi and Aliha,2021). Based on these works, additive type and content has essential and significant influence on the load carrying capacity and integrity of concrete for both before and after post-peak stages and for all loading modes (i.e. mode I, mode II, mode III, mixed mode I/II and mixed mode I/III).

As a review of the related literature confirmed the necessity of conducting a comprehensive study on the internal structure of the fracture process zone, as well as on the effects of such factors as the fiber content and the maximum aggregate size on the fracture behavior of the SCC under pure and mixed modes 1 and 3, this study examined the effects of the largest aggregate size on the fracture behavior of the SFRSCC using the three-point bending test on ENDB samples, and found the fracture toughness under pure and mixed modes I and III.

2. Test configuration

ENDB samples have a simple structure, the loading conditions under pure mode I and pure mode III and mix mode I and III are shown in Fig. 1(radius R, central notch depth a, on 2 supports 2L apart).

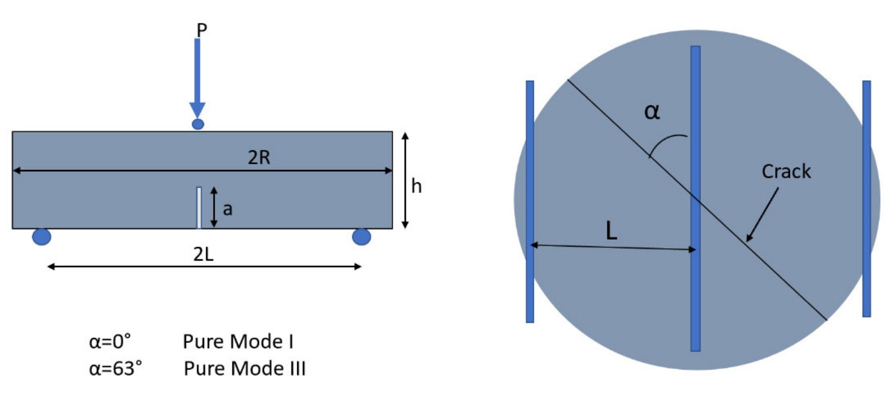

Fig. 1. Shape of ENDB notched specimens and loading conditions.

The loading, in pure mode I, is fully aligned with the crack and is quite symmetrical, and rotating angle α from 0° to 63° for different values of a/h and L/R ratios enables creating mixed modes I and III and pure mode I and III (the reader may please refer to Aliha et al. 2015, Bahmani et al. 2021 for more details on simulations and FE analyses). The fracture toughness are found for pure modes I and III and effective SIF (K_{IC}, K_{IIIC} and K_{eff}) as follows:

$$K_{IC} = \frac{6PS\sqrt{\pi a}}{RB^2} Y_I(a/h, L/R, \alpha) \quad (1)$$

$$K_{IIIC} = \frac{6PS\sqrt{\pi a}}{RB^2} Y_{III}(a/h, L/R, \alpha) \quad (2)$$

$$K_{eff} = \sqrt{(K_{IC})^2 + (K_{IIIC})^2} \quad (3)$$

where Y_I and Y_{III} are geometric factors, P is the applied load and a/h and L/R can be found in Aliha et al., (2015), for each crack inclination angle under pure modes I and III loading conditions. Mixity parameter (M^e) expresses the relative contribution of modes I and III and is defined as follows:

$$M^e = \frac{2}{\pi} tan^{-1}\left(\frac{Y_{IIIC}}{Y_{IC}}\right) \quad (4)$$

Values of Y_I, Y_{III} and M^e are listed in Table 1.

Table 1. Corresponding values of YI and YIII under all mix mode

α	Y_I	Y_{III}	M^e
0°	0.4	0	1
20°	0.325	0.049	0.905
30°	0.25	0.063	0.843
50°	0.15	0.07	0.626
63°	0	0.0615	0

3. Fracture toughness test

3.1. Materials

To investigate the fracture toughness, this study used:
1) loadings under pure and mixed modes I and III
2) coarse aggregates (broken natural stone) with dmax = 9.5, 12.5 and 19 mm and specific gravity = 2.88 3) fine aggregates with constant fineness modulus = 2.8
4) ordinary Type II Portland cement
5) modified carboxylate-based superplasticizer (SIA162 AND pr-EN 934-2) for fresh concrete ductility according to EFNARK (2005)
6) stone powder (to improve the mixture viscosity)
7) w/c = 0.45 (fixed in all mix desigen)
8) 30 mm-long, hooked-end, low-strength fibers (SF=0.1, 0.3, and 0.5%), 7.85 density, it is shown in Fig.2

Table 2. Specification of concrete mixing design and results of fresh concrete

Materials		Weight (kg/m^3)							
		SCCF1	SCCF2	SCCF3	SCCF4	SCCF5	SCCF6	SCCF7	SCCF8
cement		425	425	425	425	425	425	425	425
Sf(%)		0.3	0.3	0.3	0.3	0.3	0.3	0.1	0.5
sand		750	750	750	750	750	750	750	750
Coars aggregate	4.75-9.5(mm)	750	300	300	750	300	300	750	300
	9.5-12.5(mm)	-	450	300	-	450	300	-	450
	12.5-19 (mm)	-	-	150	-	-	150	-	-
Limestone powder		182	182	182	182	182	182	182	182
Super viscose(lit)		4250	4250	4250	4250	4250	4250	4250	4250
Concrete fresh properties									
Flow time(sec)		3.0	2.98	3.01	2.9	3.01	3.01	3.0	2.8
Slump flow(mm)		750	740	770	680	750	640	680	700
L-Box(h_2/h_1)		0.88	0.87	0.9	0.9	0.89	0.9	0.91	0.89
w/c		0.42	0.42	0.42	0.52	0.52	0.52	0.52	0.52

Fig. 2. Hooked end steel fiber

A total of 8 mix designs were made, the specifications of which are listed in Table 2.

3.2. Specimen fabrication

To make the ENDB samples, similar to that of the Brazilian test, a 150 * 300 mm cylinder was cut into several 40 mm-thick pieces (Fig. 3), each of which was, then, equipped with a 4 mm (wide) and 20 mm (length) notch along its axis using a cutting machine. The 28-day samples were tested under the strain control testing machine with a constant loading rate of 1 mm/min (Fig. 4), the crack angle was rotated relative to the loading axis to check the samples under pure and mixed modes I and III (Aliha et al., 2015) and load-displacement curves were recorded for all the samples with 0.1-0.5% fibers, 9.5-19 mm largest nominal aggregate size and 0, 20, 30, 50 and 63° crack deflection angles. Fig. 4 shows the loading conditions and Fig. 5 shows the sample failure under different loading modes.

Fig. 3. Steps of preparation and cutting of disc shape specimens

Fig. 4. Different loading modes for the ENDB specimens

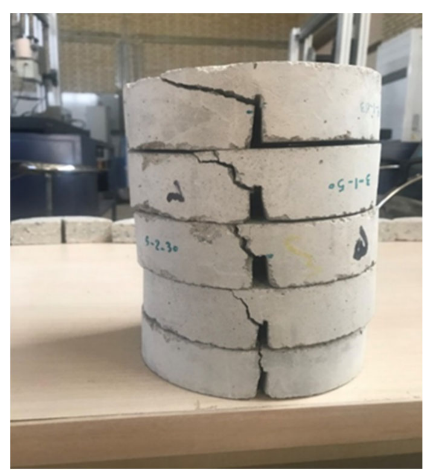

Fig. 5. Fracture paths of ENDB specimens in pure and mix mode I/III

4. Results and discussion

The fabricated samples were subjected to a three-point bending test at a loading speed of 1 mm/min. The results of maximum forces and fracture toughness for mode I and mode III and mix modes I and III for 8 different mixing designs are shown in Table 4. The results show that the maximum load decreases by moving from pure mode III to pure mode I. Also, the changes in fracture toughness for mode I and mode III and mix modes against variation in aggregate size for two water-cement ratios of 0.42 and 0.52 are shown in Fig. 6 and Fig. 7, respectively; as shown in Fig. 6, the highest fracture toughness is related to mode I and the lowest is related to mode III. This behavior has also been reported by previous researchers (Aliha et al., (2018) and Mansourian et al., (2018)). In these figures, increasing dmax to 12.5 mm first increases the fracture toughness and then decreases it. The behavior of the fracture surface and ITZ depends on the aggregate-fiber variations; in fibreless concretes, an increase in the aggregate size increases the fracture energy (Sadrmomtazi et al., 2020), but the presence of fibers and increasing the aggregate size can disturb the fracture surface and reduce the maximum load (Ghasemi et al., 2018). This trend is a bit different at w/c = 0.52, which is shown in Figure 7. Comparing Figs. 6 and 7 reveals that an increase in w/c will reduce the fracture toughness, which has also been reported by other researchers (Hoseini et al., 2022, 2023; Rahmani et al., 2020).

Table 3. Maximum forces and fracture toughness for different failure modes

	α=0°				α=20°				α=30°			
	kN	MPa.m^0.5			kN	MPa.m^0.5			kN	MPa.m^0.5		
Mix No	Pcr (ave)	K_I	K_{III}	K_{eff}	Pcr (ave)	K_I	K_{III}	K_{eff}	Pcr (ave)	K_I	K_{III}	K_{eff}
SCCF1	1.76275	0.629043	0	0.629043	2.27165	0.65865	0.099304	0.666094	2.5997	0.57982	0.146115	0.597947
SCCF2	1.9681	0.702323	0	0.702323	2.2747	0.659534	0.099437	0.666988	2.59965	0.579809	0.146112	0.597935
SCCF3	1.76885	0.63122	0	0.63122	1.9099	0.553763	0.08349	0.560021	2.21645	0.494342	0.124574	0.509797
SCCF4	1.7045	0.608257	0	0.608257	1.99265	0.577756	0.087108	0.584285	2.67325	0.596224	0.150248	0.614864
SCCF5	1.5635	0.55794	0	0.55794	1.84	0.533496	0.080435	0.539525	2.38815	0.532637	0.134225	0.549289
SCCF6	1.54895	0.552748	0	0.552748	1.78995	0.518984	0.078247	0.52485	2.2134	0.493662	0.124403	0.509096
SCCF7	1.7137	0.61154	0	0.61154	2.15515	0.624871	0.094211	0.631934	2.80815	0.626311	0.15783	0.645892
SCCF8	1.77485	0.633361	0	0.633361	1.80555	0.523507	0.078929	0.529424	2.34825	0.523738	0.131982	0.540112

	α=50°				α=63°			
	kN	MPa.m^0.5			kN	MPa.m^0.5		
Mix No	Pcr (ave)	K_I	K_{III}	K_{eff}	Pcr (ave)	K_I	K_{III}	K_{eff}
SCCF1	3.46415	0.324501	0.216334	0.390001	3.458	0	0.189727	0.189727
SCCF2	4.2183	0.395145	0.26343	0.474905	6.0393	0	0.331353	0.331353
SCCF3	3.18825	0.298656	0.199104	0.35894	4.7015	0	0.257953	0.257953
SCCF4	4.99085	0.467513	0.311675	0.561881	4.5581	0	0.250086	0.250086
SCCF5	3.0227	0.283148	0.188766	0.340302	5.0491	0	0.277025	0.277025
SCCF6	3.4948	0.327372	0.218248	0.393452	2.50155	0	0.137251	0.137251
SCCF7	4.33785	0.406344	0.270896	0.488364	5.38015	0	0.295188	0.295188
SCCF8	3.878	0.363268	0.242179	0.436594	6.61565	0	0.362976	0.362976

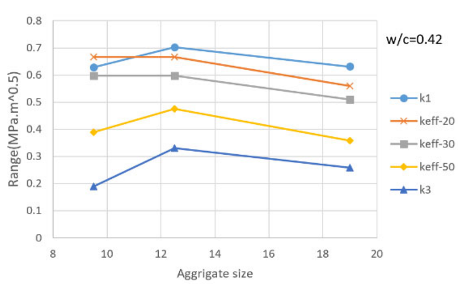

Fig. 6. Variation in fracture toughness for all failure modes versus change in aggregate size for w/c=0.42

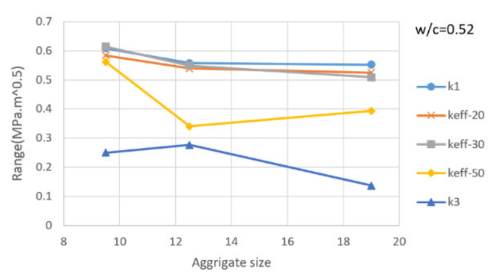

Fig. 7. Variation in fracture toughness for all failure modes versus change in aggregate size for w/c=0.52

According to Fig. 8 that shows the curves of the experimental and analytical results, the related equations (where k is the fracture toughness and d is the largest nominal aggregate size) can well model the fracture toughness.

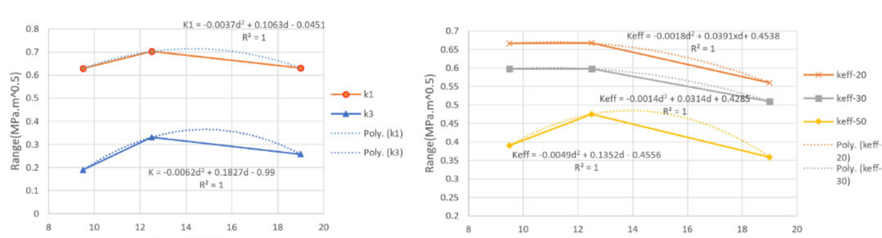

Fig. 8. Curves of estimated empirical equation of change of fracture toughness versus aggregate size

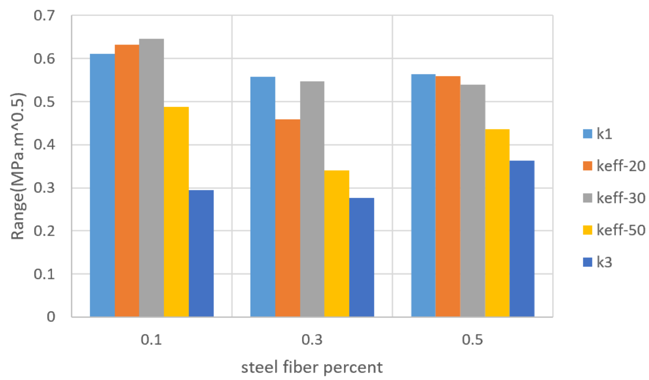

Fig. 9. Variation of Fracture toughness versus steel fiber percentage for different modes

Table 4. Empirical equations for estimating fracture toughness by changing the percentage of steel fibers

α	Mode	equation	R^2
0°	I	$K_I = 0.751f^2 - 0.5687f + 0.6609$	1
20°	Mix mode I/III	$K_{eff} = 3.4222f^2 - 2.2363f + 0.8213$	1
30°	Mix mode I/III	$K_{eff} = 1.1302f^2 - 0.9426f + 0.7288$	1
50°	Mix mode I/III	$K_{eff} = 3.0544f^2 - 1.9620f + 0.6540$	1
63°	III	$K_{III} = 1.3014f^2 - 0.6114f + 0.3433$	1

In Fig. 9 that shows the fracture toughness against steel fibers, the highest toughness is in mode 1 and the lowest toughness is related to mode 3; it is decreasing and increasing at, respectively, 0.3 and 0.5% fiber increase. In the following empirical equations that estimate the fracture toughness under pure and mixed modes I and III versus the percent steel fiber variations (Table 4), *K* is the fracture toughness and *f* is the percent of steel fibers.

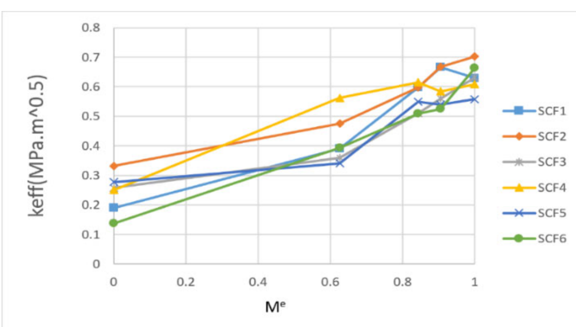

Fig.10. Variation of K_{eff} versus M^e with changes in aggregate size and water-cement ratio

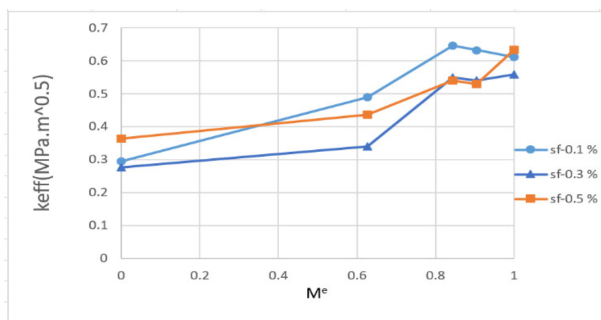

Fig. 11. Variation of K_{eff} versus M^e with change in the percentage of steel fiber

In Fig. 10 and Fig. 11 that show the fracture toughness (K_{eff}) variations against mixity parameter (M^e), with changes in the largest nominal aggregate size, w/c and percent of steel fibers, as the lowest toughness is obtained at pure mode III, the latter has a more critical state (this has been reported by previous researchers (Mousavi et al., 2021; Aliha et al., 2018). Fig. 11 shows that increasing the steel fibers does not highly improve the fracture toughness because, as mentioned before, presence of fibers in the fracture surface disturbs the fracture matrix and, hence, reduces the peak load in the load-displacement curves. Results show that in SCCF, effects of fibers are more evident after the peak load. Aliha et al. (2018), showed that in concrete containing synthetic fibers, an increase in fibers up to 0.3% increases the fracture toughness in pure modes I and III and then reduces it. It is worth noting that the fiber type and material can affect the fracture matrix and cause the fracture parameters to behave differently.

Fig. 12 shows that at w/c = 0.42, the dmax = 12.5 mm aggregate shows a better performance. According to Ghasemi et al. (2018), the dmax = 12.5 mm aggregate has the highest fracture energy. Fig. 13 shows the fracture toughness variations at w/c = 0.52 and Fig. 14 shows these variations with steel fibers. Although at 0.5% steel fibers the fracture toughness behaves better under pure modes I and III, in general, it can be concluded that increasing the steel fibers does not highly improve the concrete fracture toughness behavior.

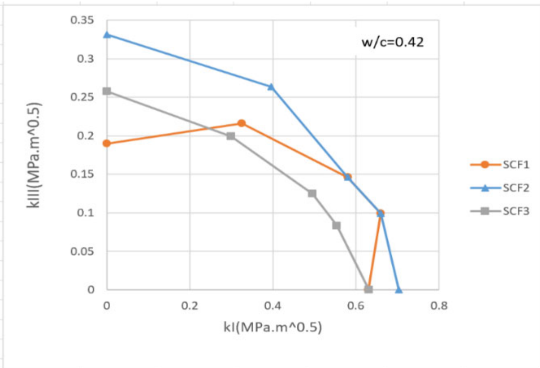

Fig.12. Effect of aggregate size on mix modes I/III fracture toughness in w/c=0.42

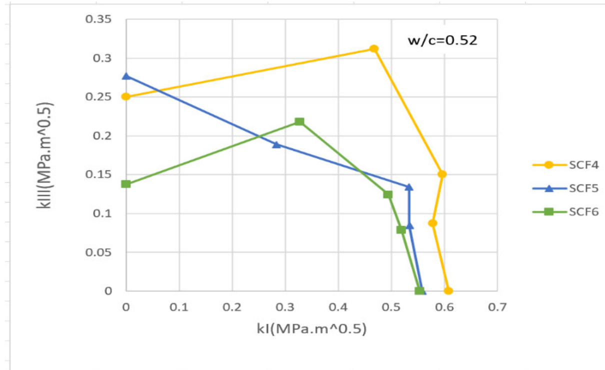

Fig. 13. Effect of aggregate size on mix modes I/III fracture toughness in w/c=0.52

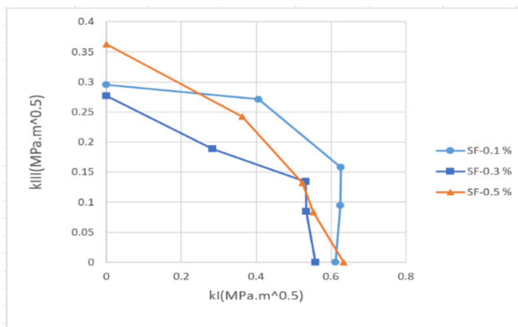

Fig. 14. Effect of percentage steel fiber on mix modes I/III fracture toughness

4.1. Examining the force-displacement curves

In Fig. 15 that shows the force-displacement curves for pure and mixed modes I and III with increasing steel fibers in the SCCF, the location of fibers in the fracture surface reduces the maximum load in most cases. Madandost et al. (2015), showed that in SCCF, an increase in steel fibers reduced the compressive strength, but the major effects of fibers were after the maximum load that absorbed energy. The oblique fracture angle in mixed modes means their better fiber effects than in pure mode I.

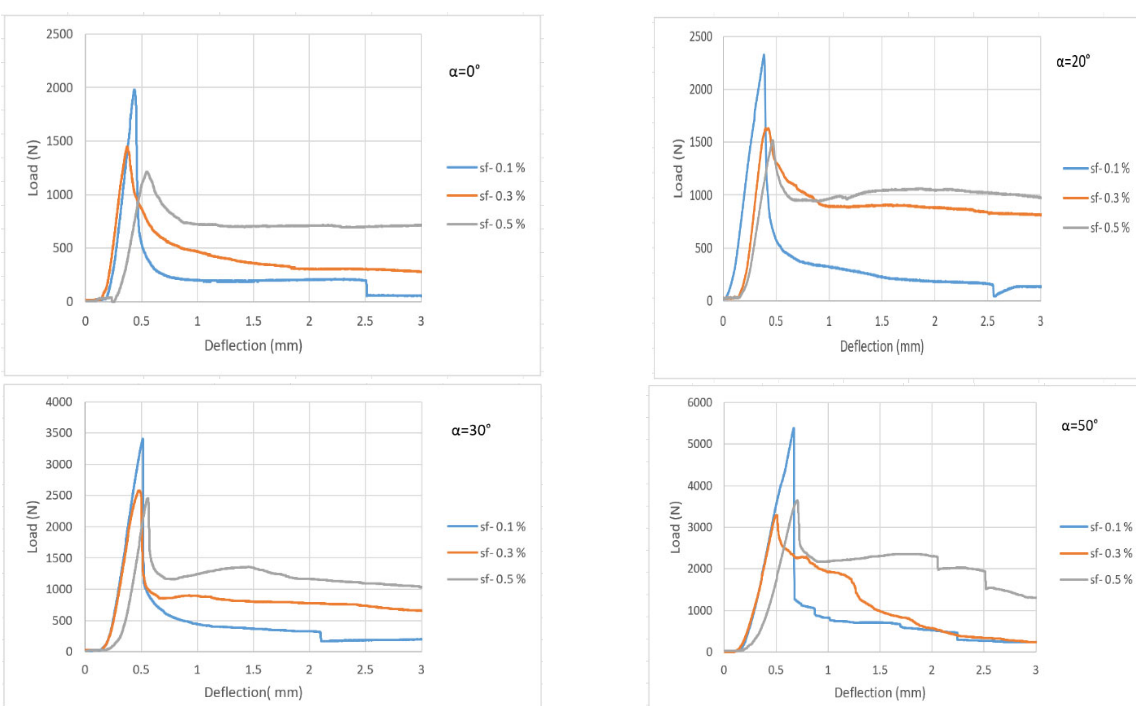

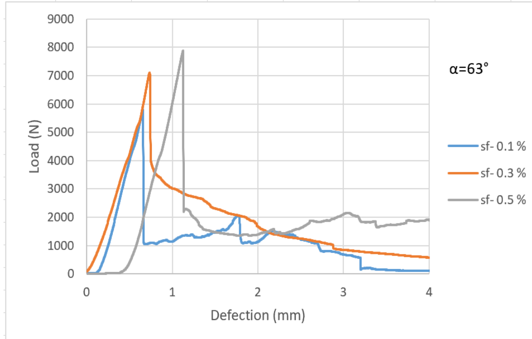

Fig. 15. Load-deflection curves for pure mode I and pure mode III and mix modes I/III with change of percentage of steel fibers

Fig. 16 shows the fracture energy variations with those of the steel fibers for pure and mixed modes I and III. Some researchers (Aliha et al., 2018) have reported that in pure mode III, an increase in steel fibers leads to an increase the fracture energy; the same has happened in the Figure; as shown, the lowest fracture energy in pure mode I and the highest is related to pure mode III because cracks are oblique in this mode and involve more fibers, which increases the energy absorption.

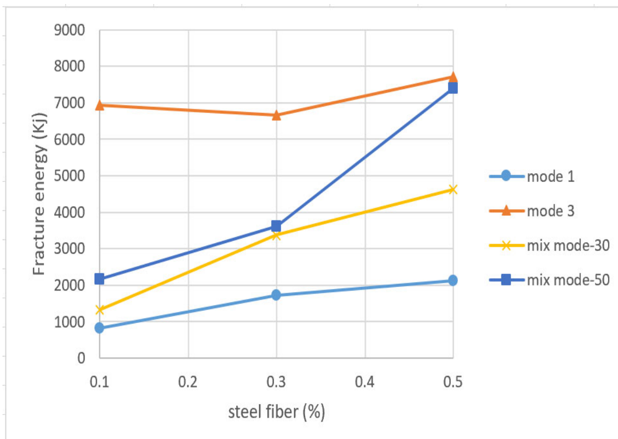

Fig. 16. Variation of fracture energy versus percentage of steel fibers

5. Conclusions

This research investigated the fracture toughness behavior of the SCCF under pure and mixed modes 1 and 3 using the largest nominal aggregate sizes of 9.5, 12.5 and 19 mm, w/c values of 0.42 and 0.52 and steel fibers of 0.1, 0.3 and 0.5%, and showed that by varying the mentioned values the most critical fracture toughness belonged to pure mode 3 and steel fibers did not highly improve the fracture toughness behavior. Changing the largest nominal aggregate size is an important parameter in SCCFs; according to the results, at the lower w/c value, the fracture toughness shows a better performance at dmax = 12.5 mm. This behavior is especially evident in pure mode 3 for both w/c values, and increasing this ratio decreases the fracture toughness. Another important conclusion shown well in the results is that fibers can increase the energy absorption for ruptures outside the crack plane, especially at the post peak.

References

Akcay, B., Agar-Ozbek, A. S., Bayramov, F., Atahan, H. N., Sengul, C., & Tasdemir, M. A. (2012). Interpretation of aggregate volume fraction effects on fracture behavior of concrete. *Construction and Building Materials*, *28*(1), 437-443.

Alberti, M. G., Enfedaque, A., & Gálvez, J. C. (2015). Comparison between polyolefin fibre reinforced vibrated conventional concrete and self-compacting concrete. *Construction and Building Materials*, *85*, 182-194.

Al-Hadithi, A. I., Noaman, A. T., & Mosleh, W. K. (2019). Mechanical properties and impact behavior of PET fiber reinforced self-compacting concrete (SCC). *Composite Structures*, *224*, 111021.

Aliha, M. R. M., Bahmani, A., & Akhondi, S. (2015). Determination of mode III fracture toughness for different materials using a new designed test configuration. *Materials & Design*, *86*, 863-871.

Aliha, M. R. M., Bahmani, A., & Akhondi, S. (2016). A novel test specimen for investigating the mixed mode I+ III fracture toughness of hot mix asphalt composites–Experimental and theoretical study. *International Journal of Solids and Structures*, *90*, 167-177.

Aliha, M. R. M., Sarbijan, M. J., & Bahmani, A. (2017). Fracture toughness determination of modified HMA mixtures with two novel disc shape configurations. *Construction and Building Materials*, *155*, 789-799.

Aliha, M. R. M., Razmi, A., & Mansourian, A. (2017). The influence of natural and synthetic fibers on low temperature mixed mode I+ II fracture behavior of warm mix asphalt (WMA) materials. *Engineering Fracture Mechanics*, *182*, 322-336.

Aliha, M. R. M., Razmi, A., & Mousavi, A. (2018). Fracture study of concrete composites with synthetic fibers additive under modes I and III using ENDB specimen. *Construction and Building Materials*, *190*, 612-622.

Aliha, M. R. M., Imani, D. M., Salehi, S. M., Shojaee, M., & Abedi, M. (2022b). Mixture optimization of epoxy base concrete for achieving highest fracture toughness and fracture energy values using Taguchi method. *Composites Communications*, *32*, 101150.

Aliha, M. R. M., reza Karimi, H., & Abedi, M. (2022a). The role of mix design and short glass fiber content on mode-I cracking characteristics of polymer concrete. *Construction and Building Materials*, *317*, 126139.

Asdollah-Tabar, M., Heidari-Rarani, M., & Aliha, M. R. M. (2021). The effect of recycled PET bottles on the fracture toughness of polymer concrete. *Composites Communications*, *25*, 100684.

Beigi, M. H., Berenjian, J., Omran, O. L., Nik, A. S., & Nikbin, I. M. (2013). An experimental survey on combined effects of fibers and nanosilica on the mechanical, rheological, and durability properties of self-compacting concrete. *Materials & Design*, *50*, 1019-1029.

Beygi, M. H., Kazemi, M. T., Amiri, J. V., Nikbin, I. M., Rabbanifar, S., & Rahmani, E. (2014). Evaluation of the effect of maximum aggregate size on fracture behavior of self compacting concrete. *Construction and Building Materials*, *55*, 202-211.

Daneshfar, M., Hassani, A., Aliha, M. R. M., & Berto, F. (2017). Evaluating mechanical properties of macro-synthetic fiber-reinforced concrete with various types and contents. *Strength of Materials*, *49*, 618-626.

Daneshfar, M., Hassani, A., Aliha, M. M., & Berto, F. (2022). Investigating Flexural Performance of Fiber-Reinforced Concrete with Different Contents and Types of Macrosynthetic Fiber. *Strength of Materials*, *54*(4), 650-661.

Daneshfar, M., Hassani, A., Aliha, M. R. M., & Sadowski, T. (2023a). Assessment of the Specimen Size Effect on the Fracture Energy of Macro-Synthetic-Fiber-Reinforced Concrete. *Materials*, *16*(2), 673.

Daneshfar, M., Hassani, A., Aliha, M. R. M., Sadowski, T., & Karimi, A. (2023b). Experimental Model for Study of Thickness Effect on Flexural Fatigue Life of Macro-Synthetic-Fiber-Reinforced Concretes. *Buildings*, *13*(3), 642.

FNARC, Concrete, S. C. (2005). The European guidelines for self-compacting concrete. BIBM, *et al*, *22*, 563.

El-Dieb, A. S. (2009). Mechanical, durability and microstructural characteristics of ultra-high-strength self-compacting concrete incorporating steel fibers. *Materials & Design*, *30*(10), 4286-4292.

Fakhri, M., Yousefian, F., Amoosoltani, E., Aliha, M. R. M., & Berto, F. (2021). Combined effects of recycled crumb rubber and silica fume on mechanical properties and mode I fracture toughness of self-compacting concrete. *Fatigue & Fracture of Engineering Materials & Structures*, *44*(10), 2659-2673.

Ferdosian, I., & Camões, A. (2021). Mechanical performance and post-cracking behavior of self-compacting steel-fiber reinforced eco-efficient ultra-high performance concrete. *Cement and Concrete Composites*, *121*, 104050.

Ferrara, L., Park, Y. D., & Shah, S. P. (2007). A method for mix-design of fiber-reinforced self-compacting concrete. *Cement and concrete research*, *37*(6), 957-971.

Ghasemi, M., Ghasemi, M. R., & Mousavi, S. R. (2018). Investigating the effects of maximum aggregate size on self-compacting steel fiber reinforced concrete fracture parameters. *Construction and Building Materials*, *162*, 674-682.

Ghasemi, M., Ghasemi, M. R., & Mousavi, S. R. (2019). Studying the fracture parameters and size effect of steel fiber-reinforced self-compacting concrete. *Construction and Building Materials*, *201*, 447-460.

Gu, X., Cheng, T., Zhang, F., & Aliha, M. R. M. Experimental and theoretical framework for illustrating the dependency of fracture toughness with tensile, bending, and compression loading in asphaltic samples. *Fatigue & Fracture of Engineering Materials & Structures*. https://doi.org/10.1111/ffe.14077

Haghighatpour, P. J., & Aliha, M. R. M. (2022). Effect of marshal and gyratory compaction methods on cracking characteristics of hot mix asphalt concrete materials under all three basic modes of fracture. *Theoretical and Applied Fracture Mechanics*, *117*, 103207.

Haghighatpour, P. J., Aliha, M. R. M., & Keymanesh, M. R. (2018). Evaluating mode I fracture resistance in asphalt mixtures using edge notched disc bend ENDB specimen with different geometrical and environmental conditions. *Engineering Fracture Mechanics*, *190*, 245-258.

He, J., Liu, L., Yang, H., & Aliha, M. R. M. (2022). Using two and three-parameter Weibull statistical model for predicting the loading rate effect on low-temperature fracture toughness of asphalt concrete with the ENDB specimen. *Theoretical and Applied Fracture Mechanics*, *121*, 103471.

Hoseini, S. O., Mousavi, S. R., Sohrabi, M. R., & Ghasemi, M. (2023). Using beam and ENDB specimens to evaluate fracture characteristics of wavy steel fiber-reinforced self-compacting concrete containing different coarse aggregate volumes. *Fatigue & Fracture of Engineering Materials & Structures*, *46*(5), 1669-1686.

Hoseini, S. O., Sohrabi, M. R., Mousavi, S. R., & Ghasemi, M. (2022). Effects of coarse aggregate and wavy steel fiber volumes on the critical stress intensity factors of modes I and III cracks in self-compacting concrete using ENDB specimens. *Theoretical and Applied Fracture Mechanics*, *121*, 103421.

Iqbal, S., Ali, A., Holschemacher, K., & Bier, T. A. (2015). Mechanical properties of steel fiber reinforced high strength lightweight self-compacting concrete (SHLSCC). *Construction and Building Materials*, *98*, 325-333.

Karamzadeh, N. S., Aliha, M. R. M., & Karimi, H. R. (2022). Investigation of the effect of components on tensile strength and mode-I fracture toughness of polymer concrete. *Arabian Journal of Geosciences*, *15*(13), 1213.

Karimi, H. R., Aliha, M. R. M., Ebneabbasi, P., Salehi, S. M., Khedri, E., & Haghighatpour, P. J. (2023a). Mode I and mode II fracture toughness and fracture energy of cement concrete containing different percentages of coarse and fine recycled tire rubber granules. *Theoretical and Applied Fracture Mechanics*, *123*, 103722.

Karimi, H. R., Aliha, M. R. M., Khedri, E., Mousavi, A., Salehi, S. M., Haghighatpour, P. J., & Ebneabbasi, P. (2023b). Strength and cracking resistance of concrete containing different percentages and sizes of recycled tire rubber granules. *Journal of Building Engineering*, *67*, 106033.

Karimi, H.R, & Aliha, M. R. M. (2021). Statistical assessment on relationship between fracture parameters of plain and fiber reinforced polymer concrete materials. *Composites Communications*, *28*, 100969.

Li, J., Zhao, E., Niu, J., & Wan, C. (2021). Study on mixture design method and mechanical properties of steel fiber reinforced self-compacting lightweight aggregate concrete. *Construction and Building Materials*, *267*, 121019.

Madandoust, R., Ranjbar, M. M., Ghavidel, R., & Shahabi, S. F. (2015). Assessment of factors influencing mechanical properties of steel fiber reinforced self-compacting concrete. *Materials & Design*, *83*, 284-294.

Mansourian, A., Hashemi, S., & Aliha, M. R. M. (2018). Evaluation of pure and mixed modes (I/III) fracture toughness of Portland cement concrete mixtures containing reclaimed asphalt pavement. *Construction and Building Materials*, *178*, 10-18.

Motamedi, H., Fazaeli, H., Aliha, M. R. M., & Amiri, H. R. (2020). Evaluation of temperature and loading rate effect on fracture toughness of fiber reinforced asphalt mixture using edge notched disc bend (ENDB) specimen. *Construction and Building Materials*, *234*, 117365.

Mousavi, S. M., Ranjbar, M. M., & Madandoust, R. (2019). Combined effects of steel fibers and water to cementitious materials ratio on the fracture behavior and brittleness of high strength concrete. *Engineering Fracture Mechanics*, *216*, 106517.

Mousavi, S. R., Afshoon, I., Bayatpour, M. A., TQ, A. D., & Miri, M. (2021). Effect of waste glass and curing aging on fracture toughness of self-compacting mortars using ENDB specimen. *Construction and Building Materials*, *282*, 122711.

Najjar, S., Moghaddam, A. M., Sahaf, A., & Aliha, M. R. M. (2020). Low temperature fracture resistance of cement emulsified asphalt mortar under mixed mode I/III loading. *Theoretical and Applied Fracture Mechanics*, *110*, 102800.

Najjar, S., Moghaddam, A. M., Sahaf, A., & Aliha, M. R. M. (2022a). Mixed mode-I/II fatigue performance of Cement Emulsified Asphalt Mortar: Experimental and statistical analysis at intermediate temperature. *Construction and Building Materials*, *350*, 128835.

Najjar, S., Moghaddam, A. M., Sahaf, A., & Aliha, M. R. M. (2022b). Experimental and statistical exploring for mixed-mode (I&II) fracture behavior of cement emulsified asphalt mortar under freeze–thaw cycles and aging condition. *Theoretical and Applied Fracture Mechanics*, *122*, 103643.

Najjar, S., Moghaddam, A. M., Sahaf, A., & Aliha, M. R. M. (2022c). Aging effect on the mixed-mode (I/III) fracture toughness of cement emulsified asphalt composite: Experimental and statistical investigation. *Engineering Fracture Mechanics*, *264*, 108292.

Najjar, S., Moghaddam, A. M., Sahaf, A., & Aliha, M. R. M. (2023). Mixed mode (I&III) fracture behavior of cement emulsified asphalt mortar under freeze and thaw cycles. *Theoretical and Applied Fracture Mechanics*, 103952.

Picazo, A., Gálvez, J. C., Alberti, M. G., & Enfedaque, A. (2018). Assessment of the shear behaviour of polyolefin fibre reinforced concrete and verification by means of digital image correlation. *Construction and Building Materials*, *181*, 565-578.

Pirmohammad, S., & Bayat, A. (2016). Characterizing mixed mode I/III fracture toughness of asphalt concrete using asymmetric disc bend (ADB) specimen. *Construction and Building Materials*, *120*, 571-580.

Rahmani, E., Sharbatdar, M. K., & Beygi, M. H. A. (2020). The effect of water-to-cement ratio on the fracture behaviors and ductility of Roller Compacted Concrete Pavement (RCCP). *Theoretical and Applied Fracture Mechanics*, *109*, 102753.

Rooholamini, H., Hassani, A., & Aliha, M. R. M. (2018a). Evaluating the effect of macro-synthetic fibre on the mechanical properties of roller-compacted concrete pavement using response surface methodology. *Construction and building materials*, *159*, 517-529.

Rooholamini, H., Hassani, A., & Aliha, M. R. M. (2018b). Fracture properties of hybrid fibre-reinforced roller-compacted concrete in mode I with consideration of possible kinked crack. *Construction and Building Materials*, *187*, 248-256.

Sadrmomtazi, A., Lotfi-Omran, O., & Nikbin, I. M. (2020). Influence of cement content and maximum aggregate size on the fracture parameters of magnetite concrete using WFM, SEM and BEM. *Theoretical and Applied Fracture Mechanics*, *107*, 102482.

Siddique, R., Nanda, V., Kadri, E. H., Khan, M. I., Singh, M., & Rajor, A. (2016). Influence of bacteria on compressive strength and permeation properties of concrete made with cement baghouse filter dust. *Construction and Building Materials*, *106*, 461-469.